# Implementation of the Enhanced Binary-SIME method for Finding Transient Stability Limits with PSS/E™

H.M. Tan, *Student Member, IEEE*, D.J. Vowles, *Member, IEEE* and R. Zivanovic, *Member, IEEE*

***Abstract*-- The Enhanced Binary-Single Machine Infinite bus Equivalent (Binary-SIME) method is an enhancement of the SIME method. It provides a robust and flexible approach to searching for the transient stability limits (TSLs) in a fully detailed model of a multi-machine power system. This paper describes the modular implementation of the Binary-SIME method with the PSS/E™ time domain simulation package. Extension to incorporate alternative search approaches is facilitated by the modular architecture. The Binary-SIME search implementation is applied to the IEEE simplified model of the Australian power system to search for power transfer limits (PTLs) and critical clearing times (CCTs). The Binary-SIME method is compared with the binary search method in the search for TSLs.**

***Index Terms*—Power System Transient Stability, Reliability, Security Assessment, Simulation Software**

## I. NOMENCLATURE

| | |
|---|---|
| CT | Clearing Time; |
| CCT | Critical Clearing Time |
| ESC | Early Stop Criterion |
| k | search iteration number |
| $\eta$ | SIME stability margin |
| MG | Machine Group |
| OMIB | One Machine Infinite Bus |
| PTL | Power Transfer Limit; |
| SIME | Single Machine Equivalent |
| SI | SIME Search Iteration start |
| SE | SIME Search iteration Exit |
| t | the $i^{th}$ time domain simulation step |
| TDS | Time Domain Simulation |
| TSL | Transient Stability Limit |

## II. INTRODUCTION

The SIME method [1] is based on the derivation of the response of an equivalent One Machine Infinite Bus (OMIB) system from the transient responses of all the machines in a fully detailed model of a multi-machine system. This approach enables the determination of transient stability margins which can be used to predict the forward-swing transient stability limit. The OMIB response also enables the use of early stop criteria (ESC) which allows early identification of forward-swing (in)stability. Prediction of the TSL based on the margin information, together with the application of the ESC, enables accelerated computation of the TSL.

The Binary-SIME search technique [2] enhances the robustness of the basic SIME algorithm by switching to a binary search step whenever the SIME limit prediction cannot be applied. This occurs during search initialization, or where the SIME limit prediction fails to converge, or if a system scenario is too (un)stable for the SIME margin to be calculated.

The enhanced Binary-SIME method for limit searching is peripheral to the TDS software and does not require access to, or modification of, the TDS source code. The modular implementation of the Binary-SIME algorithm with the Siemens PSS/E™ software [3] is depicted in Fig. 1. The proposed implementation is designed such that alternative limit search methods can be readily incorporated. Besides producing TSLs the Binary-SIME method provides transient-stability margin information which may be useful for sensitivity analysis and control.

In III the implementation of the enhanced Binary-SIME algorithm is described. In IV and V the methodology to search for the forward-swing and multi-swing TSL is explained. The Binary-SIME and binary search algorithms are applied to search for TSLs on the IEEE simplified South East (SE) Australian Power System model [4] which is described in VI. Results of the investigation are discussed in VII.

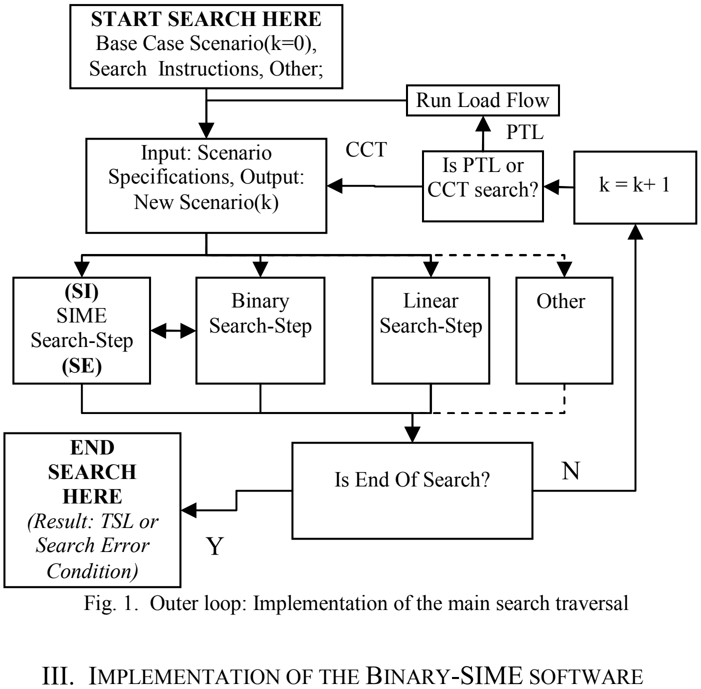

Fig. 1. Outer loop: Implementation of the main search traversal

## III. IMPLEMENTATION OF THE BINARY-SIME SOFTWARE

The Binary-SIME implementation is composed of an outer loop to produce the next search scenario (Fig. 1) and an inner loop to execute the Binary-SIME algorithm for each scenario (Fig. 2). The search is automated using PSS/E™ automation

978-1-4244-2235-7/09/$25.00 ©2009 IEEE

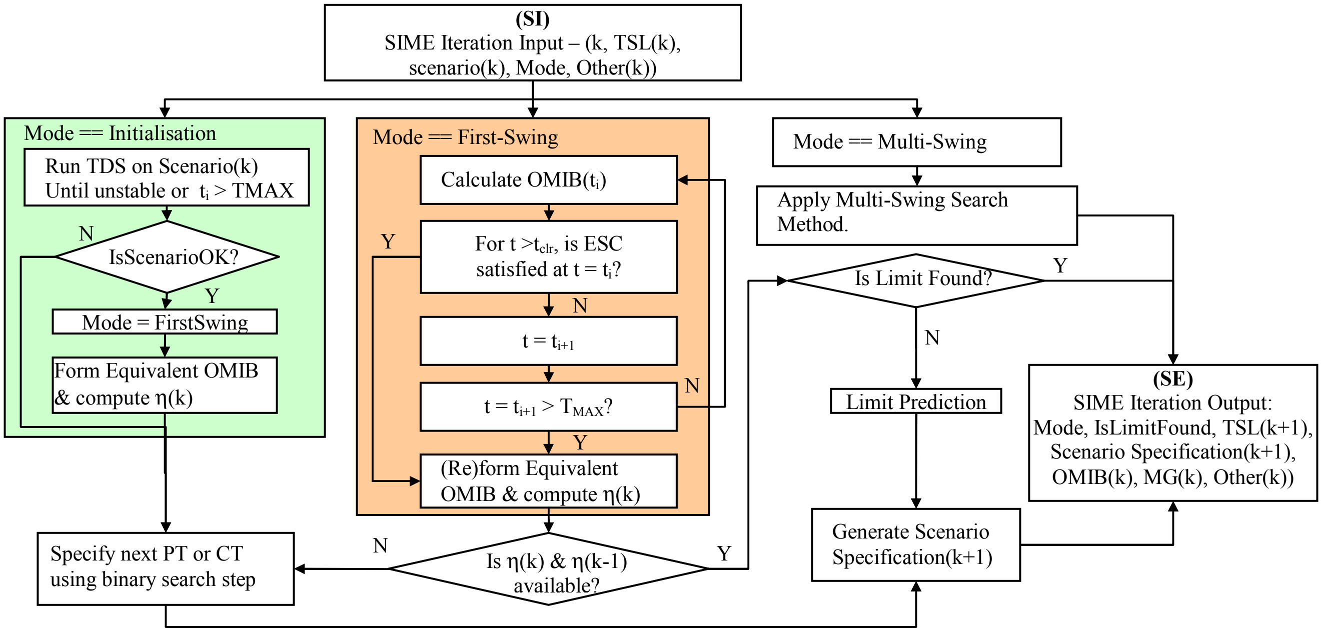

Fig. 2. Inner Loop: Implementation of the Binary-SIME search iteration algorithm

facilities [3]. The outer loop of the search is implemented in Python [3, 5], and the inner loop is implemented as a PSS/E™ user-defined model using the Fortran 95 language [3, 6]. The model is compiled and linked into the PSS/E™ software. Fortran 95 modules are used to implement the inner loop of the algorithm. This allows variations in the algorithm, such as alternative ESC, to be implemented and explored in a straight forward manner. Dynamically allocatable storage is used to facilitate efficient handling of the large volumes of data and for analyzing power systems of widely differing sizes. The current software implementation has been designed with both research and production use in mind. Facilities include:

- flexible text based configuration of a TSL search
- comprehensive TSL search summaries
- options to save all generator, OMIB and Centre of Inertia [7] (COI) data into compact binary files. These can be easily translated for viewing with MATLAB® [8]
- enable/ disable use of the SIME ESC during the search.
- record the wall-clock execution time and simulated time, for each search scenario individually and cumulatively.
- options to select the level and detail of diagnostic and error reporting
- options to redirect search traversal based on forward- or multi-swing search boundaries
- options to specify machine groups (see IV.B.) for SIME OMIB calculations

## IV. SEARCH FOR THE FORWARD SWING LIMIT

As described in [2] and Fig. 2. the purpose of the initialization and first-swing phases of the Binary-SIME search is to locate the forward-swing stability limit. The implementation of these phases is described in the following sections.

### *A. Stability Assessment – Stopping Criteria*

For all scenarios the rotor-angles of all machines with respect to the COI angle is examined at each time step of the TDS. If the rotor angle of any machine deviates by more than 180° from the COI angle then the system is declared unstable. Stable scenarios are simulated for a full integration period (i.e. 10 seconds in this paper). During the initialization and first-swing phases of the Binary-SIME search the SIME forward-swing ESC may be applied to terminate the simulation earlier. The ESC identifies forward-swing stability. The ESC are based on the application of the Equal Area Criterion to the OMIB accelerating-power – rotor-ange response in the period immediately following the application of the fault and whilst the rotor-speed is above synchronous speed (i.e. the forward swing) [1,2,9].

### *B. Machine grouping*

To apply SIME assessment and calculate the OMIB responses the system must be divided into two machine groups (MGs). The MGs can be determined from the first unstable scenario [2]. In the enhanced-SIME implementation there is an option to update the MGs whenever an unstable scenario is encountered during the search. However, results of TSLs on the simplified Australian system and from [9] indicate that the MGs should be determined from a very unstable first scenario and should not be modified during the course of the search.

### *C. SIME Margins*

The SIME margins, $\eta$, are determined from the forward-swing analysis of the OMIB power-angle response. As soon as two scenarios with valid margins (by the same MG) have been identified the SIME limit prediction can be applied.

#### *1) Unstable margin*

The unstable margin is calculated by applying the trapezoidal method to calculate the difference between the acceleration and deceleration areas of the OMIB power-angle curve[1, 2].

#### *2) Stable Margin*

Unlike the unstable margin, the stable margin cannot be calculated directly from the OMIB response. The path of the power angle curve must be extrapolated from the forward-swing return angle, $\delta_r$, to the angle of instability, $\delta_{lim}$, where the OMIB acceleration power ($P_a$) is zero (Fig. 3). A linear least squares (LLS) estimation algorithm is applied to fit a quadratic function to the OMIB power-angle response spanning from the clearing angle, $\delta_{clr}$ to $\delta_r$ [10]. An initial investigation indicates that about 400 points, equally spaced on the rotor-angle axis, yields a quadratic function which is sufficiently accurate and usually insensitive to relatively small deviations in the power-angle curve. This is the number of data points used in the paper, although it is configurable in the software. If the estimated curve does not intersect the rotor angle axis (at $P_a = 0$, for $\delta > \delta_r$ ), then the scenario is classified as to "too stable" for the purpose of margin calculation.

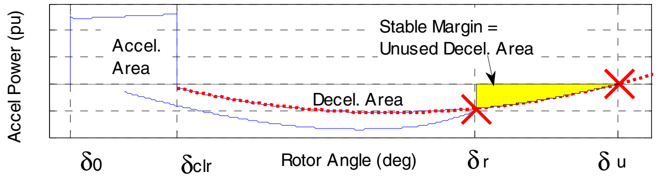

Fig.3. The power angle curve for a stable scenario. It shows the projected path of the curve to instability, and subsequent stable margin.

### D. *Search Bounds*

In the binary-SIME algorithm there are two sets of search bounds – one set of bounds applies to multi-swing stability and the other to forward-swing stability. The algorithm ensures that the forward-swing bounds are always on or within the multi-swing bounds. If the COI stopping criterion is applied to a given scenario, then in the ensuing assessment, both sets of search bounds are updated. If the ESC criterion is applied then only the forward-swing search bounds are updated.

### E. *Convergence to the Forward-Swing Limit*

The forward-swing limit is found if either one of the following conditions is satisfied:

a) $0<\eta(k)<\eta_{tol}$. [2], where $\eta(k)$ is the SIME margin of the current scenario and $\eta_{tol}$ is the search margin tolerance

b) The difference between the updated forward-swing search bounds is within the binary search tolerance. This condition is important in case the selected $\eta_{tol}$ is unrealistically low.

### F. *Detecting Failure To Converge And Redirecting The Search*

Failure of Binary-SIME search convergence is detected by the following conditions:

a) If, before the TSL is found, the reduction in the SIME margin between successive scenarios is less than a user defined threshold of $\eta_{slow}$ then the convergence rate is deemed to be too slow: i.e. convergence failure occurs if $|\eta(k)-\eta(k-1)|<\eta_{slow}$. In these studies $\eta_{slow}=\eta_{tol}$.

b) the predicted TSL is outside of the forward-swing search bounds.

If condition a) occurs then the next search step is redirected to the bisection of the forward-swing bounds. In the event of condition b) the next search step is determined by bisecting the multi-swing bounds, and the forward-swing bounds are reset to the multi-swing bounds. Following condition b) the COI stop criterion must be applied to update the multi-swing bounds to guard against a circular search traversal. It is possible that following search redirection a previously assessed scenario may be repeated. Such circumstances are recognized by the outer search loop; previous margin information can be reused without re-simulating the scenario; and snapshots of previous simulations can be recovered and continued from their last time point. If failure to converge occurs more than once then the algorithm will be completed using a binary search.

## V. MULTI-SWING PHASE

When the forward-swing limit is identified it must be assessed for multi-swing stability using the COI stability criterion. If the forward-swing limit is also multi-swing stable then the search is complete and the limit is found. Otherwise, the forward-swing limit becomes the upper search bound and the search must continue in multi-swing mode (see Fig. 2.).

As mentioned above, PSS/E™ provides the ability to recall previous simulations and to continue running them from the last simulation point. Where it is beneficial, this facility is employed in the multi-swing search phase.

The multi-swing search phase proceeds by applying the COI stability criterion to determine the multi-swing stability of scenarios which were previously assessed for forward-swing stability by the ESC. The scenarios are examined for multi-swing stability in order from the least to most stable, as originally determined by the ESC. If a previous scenario is determined to be multi-swing unstable then it replaces the upper binary search bound, otherwise it replaces the lower binary search bound. Once a multi-swing stable scenario is identified, or if all previous simulations have been examined, then the multi-swing search continues with a binary search until the TSL is found.

## VI. THE SIMPLIFIED MODEL OF THE SE AUSTRALIAN SYSTEM

The IEEE simplified model of the South-East (SE) Australian power system [4] is used to investigate the Binary-SIME search algorithm. It is a 50 Hz system that consists of 14 multi-machine power stations and represents a relatively weak longitudinal system as compared to the more tightly meshed networks found in much of Europe and the USA. As shown in the geographical layout in Fig. 4 the system comprises four weakly interconnected areas. Hence there are three inter-area modes of oscillation, as well as ten local-area modes. Each of the 14 power stations comprises between 2 to 12 identical generating units. The generator models are detailed 5th or 6th order machine models and are fitted with detailed excitation system models (including Power System Stabilizers which are necessary for system stability). The model also incorporates six Static Var Compensators, with realistic controls including current-droop compensation and susceptance limits. In the investigated cases three phase faults are applied to various lines on the South Australia (SA) to Victoria (VIC) interconnection. Fig. 5 depicts the SA and VIC components of the system in detail.

## VII. RESULTS

In this section the enhanced Binary-SIME method is applied to search for TSLs on the simplified SE Australian power system model. The results provide a comparison of the performance of the Binary-SIME algorithm with respect to the standard binary-search. They also reveal some limitations of the SIME technique and thus the necessity of reverting to binary search steps to ensure that the correct TSL is found. In the following examples all references to search time refer to the simulated time (SIM) and not the computation time.

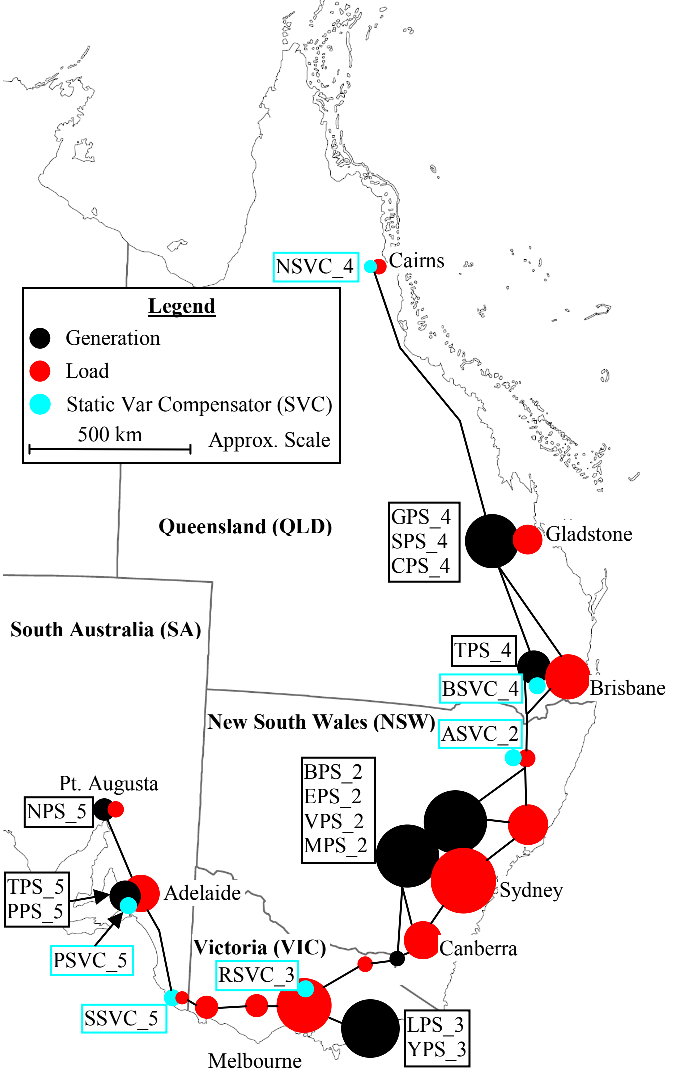

Fig. 4. A geographical representation of the simplified S-E Australian Power System. Relative magnitudes of loads and generation are indicated by the areas of the respective symbols.

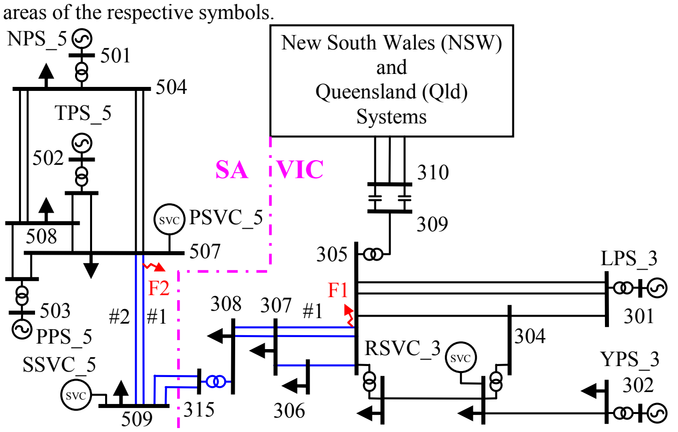

Fig. 5. The one line diagram of the SA & VIC regions of the power system. The elements of the VIC-SA interconnector are shown in blue.

The simulated time is used since it is independent of the computing hardware and transient stability program used.

## A. *Case 1.*

In this case the power transfer from Victoria to South Australia is 500 MW over the VIC-SA interconnection. A three-phase fault (F1 in Fig. 5) is applied near to the bus 305 end of transmission circuit #1 connecting bus 305 to bus 307. The fault is cleared by simultaneously tripping the circuit breakers at each end of the faulted line. Table 1 summarizes the results of a binary search for the CCT. The search tolerance is 2 ms.

A CCT search using the binary-SIME algorithm is also applied to this case, where a margin tolerance of 0.0002 rad-p.u., and search bound tolerance of 2ms are used. The search is summarized in Table 2.

TABLE 1. SUMMARY OF BINARY SEARCH FOR CCT FOR 500MW POWER TRANSFER FROM VIC-SA, FAULT APPLIED AT BUS 305

| k | CT (ms) | Stable/ Unstable | M-S Search bounds (ms) | SIM Time (s) |
|---|---|---|---|---|
| 1 | 500 | U | [0, 500] | 1.50 |
| 2 | 250 | U | [0, 250] | 1.52 |
| 3 | 125 | S | [125, 500] | 10.00 |
| 4 | 188 | U | [125, 188] | 1.69 |
| 5 | 157 | U | [125, 157] | 2.02 |
| 6 | 141 | S | [141, 157] | 10.00 |
| **7** | **CCT = 149** | **S** | **[141, 149]** | **10.00** |
| 8 | 153 | U | [149, 153] | 2.15 |
| 9 | 151 | U | [149, 151] | 2.33 |
| **Total Simulated Time (s)** | | | | 41.20 |

TABLE 2. SUMMARY OF THE BINARY-SIME SEARCH FOR CCT FOR 500MW POWER TRANSFER FROM VIC-SA, FAULT APPLIED AT BUS 305

| k | η(k-1) (rad-pu) | η(k) (rad-pu) | CT (ms) | F-S search bounds (ms) | M-S search bounds (ms) | SIM Time (s) |
|---|---|---|---|---|---|---|
| 1 | - | - | 500 | [0, 500] | [0, 500] | 1.5 |
| 2 | - | -0.19304 | 250 | [0, 250] | [0, 500] | 1.31 |
| 3 | -0.19304 | 0.048460 | 125 | [125, 250] | [0, 500] | 1.51 |
| 4 | 0.048460 | 0.002310 | 150 | [150, 250] | [0, 500] | 1.80 |
| 5 | 0.002310 | 0.001250 | 151 | [151, 250] | [0, 500] | 1.83 |
| 6 | 0.001250 | 0.000548 | 152 | [152, 250] | [0, 500] | 1.87 |
| 7 | 0.000548 | 0.000167 | 153 | [153, 250] | [0, 500] | 1.91 |
| 8 | - | - | 153 | - | [0, 153] | 0.24 |
| 9 | - | - | 152 | - | [0, 152] | 0.34 |
| 10 | - | - | 151 | - | [0, 151] | 0.50 |
| **11** | **-** | **-** | **150** | **-** | **[150, 151]** | **8.20** |
| **Total Simulated Search time (s)** | | | | | | **28.42** |

The Binary-SIME search commences in the initial search phase (see Fig. 2) between the binary search bounds of [0, 500] ms. In the first search iteration a scenario with a clearing time of 500ms is assessed. Transient instability is identified by the COI stop criteria at t=1.432s (see Fig. 6). At this time, the largest angle separation occurs between the LPS_3 generators at bus B301 and the rest of the system. This separation defines the MGs which are used for the rest of the Binary-SIME search. It is interesting to note that the system actually separates into 3 sections – SA, VIC and the rest of the system. This seems to differ from the SIME assumption that loss of synchronism is caused by the separation between two groups of machines [1].

Furthermore, it is observed from Fig. 6 that the two VIC stations, LPS_3 & YPS_3 separate together from the remainder of the system, although at the time when the machine groups are identified (i.e. t = 1.432 s) the YPS_3 machine is grouped with the remainder of the system rather than with LPS_3. This apparent inconsistency in machine grouping requires further investigation.

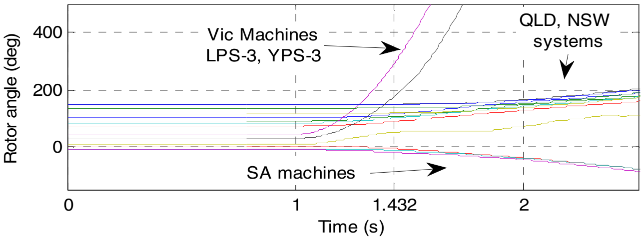

Fig. 6. Rotor Angle responses of the test system where PT is 500MW from VIC-SA, and CT is 500ms.

Since, during this first iteration, the system does not commence decelerating before synchronism is lost a stability margin cannot be determined.

Bisection is used to determine the CT of 250 ms in the second iteration. It is identified as forward-swing unstable, at t = 1.31s by application of the ESC to the OMIB response. An unstable margin is determined for this scenario, thus the Binary-SIME search can commence the first-swing phase at the next step. The CT of 125 ms of the first scenario of first-swing phase (at k = 3) is determined by a binary step. By the ESC the scenario is determined to be forward-swing stable at t = 1.51s. It provides an estimated stable margin of 0.04846 rad-pu. Since the stability margin is greater than the search tolerance the CT of the next search step is estimated from the margins of iterations 2 and 3 by interpolation to be 150ms. The process of determining forward-swing stability or instability by the ESC, calculating the SIME margin, and predicting the CCT at the next step continues for iterations 4 to 7 inclusive. At scenario 7 the calculated margin is stable and less than the search tolerance, thus the forward-swing limit is found at a CT of 153ms. The simulation for this scenario is continued, in step 8, to determine if the forward-swing limit is also multi-swing stable. The COI stop criterion determines that it is not. Thus, the multi-swing phase of the search commences with the multi-swing search bounds of [0, 153] ms.

The multi-swing search phase (see V.) commences in step 9. The simulation of the step 6 scenario (i.e. the least stable of steps 4 to 6 according to the ESC) is continued and is found to be multi-swing unstable. Similarly, in step 10 the simulation of the scenario in step 5 is continued and is found to be multi-swing unstable. Finally, in step 11, the simulation of the step 4 scenario is continued and is found to be multi-swing stable. Since the difference between the CT in steps 10 (151 ms, unstable) & 11 (150 ms, stable) is less than the binary search tolerance of 2 ms, the CCT is found to be 150 ms in step 11.

Here, the SIME limit prediction technique provides a good CCT estimate and fast convergence to the limit. The cumulative simulation time of the binary search is 41.2 s which is about 30% higher than the 28.42s total simulation time of the Binary-SIME (BSIME) search. The convergence of the two methods are compared in Fig. 7. Note that the simulation times reported are slightly skewed because the simulation is run for 1 s before applying the disturbance.

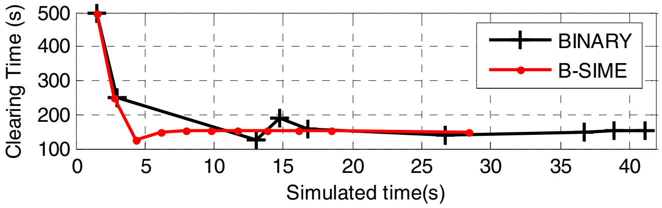

Fig. 7. A comparison of the Binary-SIME and binary searches for Case 1.

## *B. Case 2*

The system operating conditions are the same as in Case 1. In Case 2 the objective is to determine the CCT for a 3-phase fault applied at the bus 507 end of the #1 transmission circuit between buses 507 & 509 (i.e. fault F2 in Fig. 5). The fault is cleared by simultaneously tripping the circuit breakers at each end of the line. The results of a binary search for the CCT of 167 ms in this case are summarized in Table 3.

TABLE 3. SUMMARY OF THE BINARY SEARCH FOR CCT FOR 500MW POWER TRANSFER FROM VIC-SA, FAULT APPLIED AT BUS 507

| **k** | **CT (s)** | **Stable/ Unstable** | **M-S Search bounds (ms)** | **SIM Time (s)** |
|---|---|---|---|---|
| 1 | 500 | U | [0, 500] | 3.45 |
| 2 | 250 | U | [0, 250] | 10.00 |
| 3 | 125 | S | [125, 500] | 3.28 |
| 4 | 188 | U | [125, 188] | 10.00 |
| 5 | 157 | U | [125, 157] | 3.60 |
| 6 | 173 | U | [125, 173] | 10.00 |
| 7 | 165 | S | [165, 173] | 3.88 |
| 8 | 169 | U | [165, 169] | 10.00 |
| 9 | CCT = 167 | S | [167, 169] | 3.45 |
| **Total Simulated Time** | | | | 55.79 |

The results of the Binary-SIME search for the CCT for this case are summarized in Table 4.

TABLE 4. SUMMARY OF THE BINARY SEARCH FOR CCT FOR 500MW POWER TRANSFER FROM VIC-SA, FAULT APPLIED AT BUS 507

| **K** | **η(k-1) (rad-pu)** | **η(k) (rad-pu)** | **CT (ms)** | **F-S search bounds (ms)** | **M-S search bounds (ms)** | **SIM Time (s)** |
|---|---|---|---|---|---|---|
| 1 | - | - | 500 | [0, 500] | [0, 500] | 1.57 |
| 2 | - | -0.00662 | 250 | [0, 250] | [0, 500] | 1.71 |
| 3 | -0.00662 | 0.00267 | 125 | [125, 250] | [0, 500] | 1.57 |
| 4 | 0.00267 | 0.00365 | 161 | [161, 250] | [0, 500] | 1.62 |
| | **Predicted CCT: *28 ms* - Redirection using binary search bounds** | | | | | |
| 5 | 0.00365 | -0.00662 | 250 | [0, 250] | [0, 250] | 1.74 |
| 6 | -0.00662 | 0.00382 | 193 | [193, 250] | [0, 250] | 1.82 |
| 7 | 0.00382 | -0.00357 | 214 | [193, 214] | [0, 250] | 1.71 |
| 8 | -0.00357 | -0.00312 | 204 | [193, 204] | [0, 250] | 1.72 |
| | **Predicted CCT: *135 ms* - Redirection using binary search bounds** | | | | | |
| 9 | - | - | 125 | - | [125, 250] | 8.43 |
| 10 | - | - | 188 | - | [125, 188] | 3.28 |
| 11 | - | - | 157 | - | [157, 188] | 10.00 |
| 12 | - | - | 173 | - | [125,173] | 3.60 |
| 13 | - | - | 165 | - | [165, 173] | 10.00 |
| 14 | - | - | 169 | - | [165, 169] | 3.88 |
| **15** | | | **167** | | **[167, 169]** | **10.00** |
| **Total Simulated Search time** | | | | | | 62.56 |

In this example the presence of back-swing instability causes the SIME component of the search to fail. Eventually the binary search is employed to ensure that the search converges to the limit.

The search commences with the clearing time, at the upper binary search bound, of 500ms. By COI assessment it is determined to be unstable at t = 1.57 s. At this point two of the SA machines, NPS_5 and TPS_5, are identified as one MG, with the remaining machines forming the other MG. However, Fig. 8 indicates that in this scenario eventually all three SA machines lose synchronism with the remainder of the system.

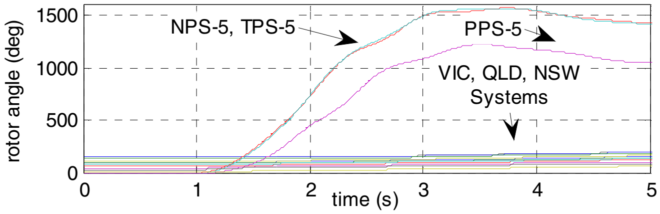

Fig. 8. The machine rotor angle responses of the full system for Case 02.

The second scenario with a CT of 250 ms, determined by bisection, is assessed as unstable by the ESC. The SIME unstable margin is determined for this scenario and the search is able to proceed to the first-swing phase. The CT in the third scenario is determined by a binary step using the forward-swing bounds to be 125 ms. It provides a stable margin, which is outside the search tolerance. Thus, interpolation of the stable margin at the current step and unstable margin of the previous step is used to estimate the CCT to be 161 ms.

The first-swing search phase proceeds with the same process described in Case 1. However, at k = 4 the CCT is estimated to be 28ms, which is outside the forward-swing bounds. Thus the Binary-SIME search must be redirected. The forward-swing bounds are reset to the multi-swing bounds of [0, 250] ms. The scenario with CT = 250ms is confirmed in the 5th step to be unstable using the COI stop criterion. The margin at 250 ms clearing time is used with the margin of the previous scenario (k = 4, CT = 161ms) to estimate the CCT of 193 ms at the next search step (k = 6). At step 6, the scenario with CT = 193 ms is assessed by the ESC to be forward-swing stable. However, this scenario is, in fact, unstable. This is where the SIME method begins to mis-direct the limit search.

Fig. 9 shows the OMIB responses of the rotor-angle, rotor-speed and accelerating power for the scenario with CT = 193 ms. It is apparent that application of the ESC shows the system is forward-swing stable at t = $t_A$ = 1.65 s. However, at t = $t_D$ = 3.6 s the rotor-speed reaches a local maximum which is sub-synchronous and at the same time the accelerating power is decreasing. Consequently, the OMIB system decelerates uncontrollably and synchronism is lost. Thus, although the OMIB system for this scenario correctly reveals that the system is unstable, the ESC which is based only on analysis of the forward swing incorrectly predicts that the system is stable.

It is instructive to examine responses of variables in the detailed system model to explain the reason for the occurrence of instability in the back-swing. Fig. 10 shows the responses of (i) the bus 509 voltage (V); (ii) the power flow in the #2 circuit from bus 509 to 507; (iii) the susceptance of the SVC SSVC_5 which is connected to bus 509 (B); and (iv) the rotor-speed of the TPS_5 machine which is connected to bus 502 (W).

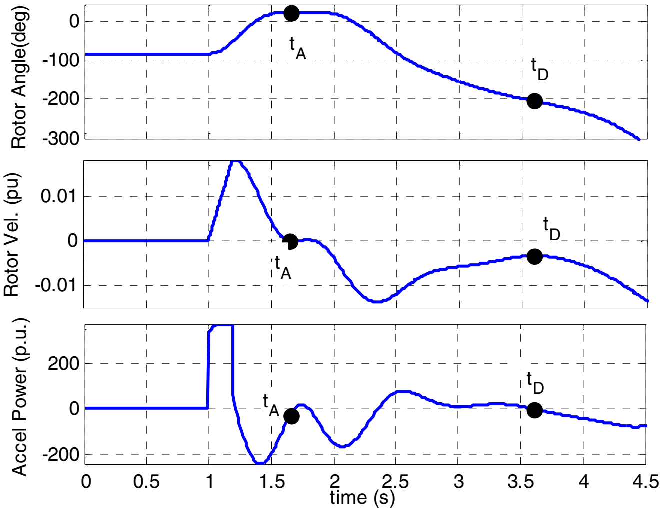

Fig. 9. The OMIB rotor angle, velocity and acceleration power responses where the fault clearing time is 193ms.

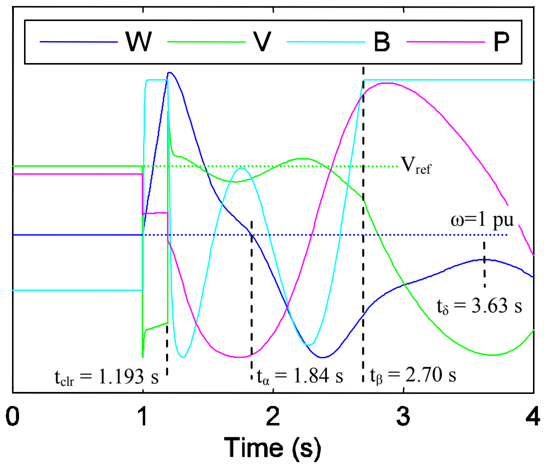

Fig 10. Time responses of: (i) the bus 509 voltage (V); (ii) the power flow in the #2 circuit from bus 509 to 507; (iii) the susceptance of the SVC SSVC_5 connected to bus 509 (B); the rotor-speed of the TPS_5 machine.

In the period immediately following the clearance of the fault the power flow from VIC to SA falls below its pre-disturbance level due to the advance in the rotor-angles of the SA machines with respect to those in the remainder of the system which occurs during the fault.

Due to the reduced power flow on the VIC to SA interconnector (P) the voltage at bus 509 (V) tends to increase above the SSVC_5 voltage set-point. The SVC AVR therefore acts to reduce the SVC susceptance (B). During the first swing following the fault, the rotors of the SA machines decelerate, slow to synchronous speed ($t_\alpha$ = 1.84 s for the TPS_5 machine) and thence continue to decelerate. Once the rotor speeds of the SA machines slow below synchronous, the power flow from VIC to SA begins to increase. As the power transfer increases the bus 509 voltage tends to decrease. The SVC responds to this voltage decrease by increasing the SVC susceptance. However, at time $t_\beta$ = 2.70s the SVC reaches its capacitive limit. As the interconnector power flow continues to increase the voltage at bus 509 continues to decline. The declining voltage is associated with a reduction in the interconnector power transfer which means that the rotor-speeds of the SA machines are unable to accelerate to synchronous speed. (The TPS_5 machine reaches a maximum rotor-speed of 0.997 pu at $t_\delta$ = 3.64s during the back-swing). The net generation deficit in SA means that its machines continue to decelerate and as a result synchronism is lost.

Instability is associated with the loss of voltage control by the SVC at bus 509. This loss of control necessarily occurs after the SA machines first decelerate to synchronous speed following the clearance of the fault. If, at the time when the SA machines first return to synchronous speed following fault clearance, the net power consumption of SA is positive then according to the forward swing early stop criteria the system is stable – which yields an incorrect diagnosis of stability in this case.

Steps k = 7 and 8 continue the search for the forward-swing limit with failure to converge eventually being identified at scenario 8, where the predicted CCT of 135ms is outside of the forward-swing search bounds. As this is the second time that convergence failure has been detected, the Binary-SIME algorithm switches to the binary search mode to complete the search.

Fig. 11. shows a comparison of the performances of the binary-SIME and the binary search methods.

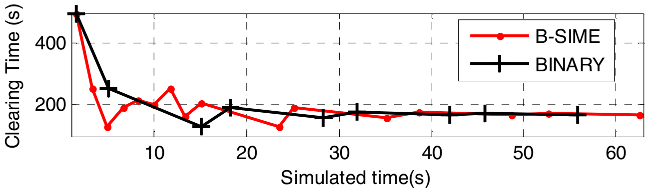

Fig. 11. Performance of the binary-SIME and binary searches for Case 2.

Due to the failure of the ESC to identify instability in the back-swing and the associated convergence failures during the forward-swing limit-search the search time of the Binary-SIME method (62.6s) was slightly greater than that required by the binary-search method (55.8s). However, the ability of the Binary-SIME search to identify the convergence failures and switch to a binary search mode means that the method does correctly identify the CCT. Furthermore, the extra search time, as compared to a binary-search, is minimized because snapshots of previous simulations in the search are recovered and continued.

### *C. Case 3*

In this case the objective is to search for the power transfer limit from VIC to SA. A three phase fault is applied at the bus 507 end of #1 transmission circuit between buses 507 and 509 (i.e. fault F2 in Fig. 5.). The fault is cleared by disconnecting the faulted circuit in 120ms. The Binary-SIME and binary search algorithms were applied to search for the power transfer limit. A summary of the binary search, run to a resolution of 5MW, is listed in Table 5. (It should be noted that when the simulations are run for an integration period of 20s, the actual PTL is revealed to be 571MW because in the case with a power transfer of 572 MW, instability occurs at approximately t = 11s.)

As with Case 2 the system is limited by back-swing instability which means the SIME component for the binary-SIME search is relatively ineffective. In this case incorrect diagnosis of stability by the forward-swing early stop criterion is evident from the first search scenario.

TABLE 5. SUMMARY OF THE BINARY AND BINARY-SIME SEARCHES FOR PTL FOR CT = 120MS, FAULT APPLIED AT BUS 507

| k | PT (MW) | Stable/ Unstable | M-S Search bounds (MW) | SIM Time (s) |
|---|---|---|---|---|
| 1 | 650 | U | [0, 650] | 1.79 |
| 2 | 325 | S | [325, 650] | 10.00 |
| 3 | 488 | S | [488, 650] | 10.00 |
| 4 | 569 | S | [569, 650] | 10.00 |
| 5 | 610 | U | [569, 610] | 3.55 |
| 6 | 590 | U | [569, 590] | 3.85 |
| 7 | 580 | U | [569, 580] | 4.26 |
| 8 | 575 | U | [569, 575] | 4.87 |
| **9** | **572** | **S** | **[572, 575]** | **10.00** |
| **Total Simulated Time** | | | | 59.78 |

The first search scenario of the Binary-SIME algorithm commences at a power transfer level of 650MW. By the COI stop criterion the system is identified to be unstable at t = 1.79s. From this point the SA machines NPS_5 and TPS_5 were identified in one MG with the machines of the remainder of the system in the other group, as in Case 2. Having identified the MGs the OMIB response is calculated for the scenario. As part of assessing the SIME margin the ESC conditions are checked for consistency. However, OMIB acceleration power and rotor velocity responses reveal, in Fig. 12, the scenario is forward-swing stable. The ESC classification contradicts the COI assessment. This is a possible indication that the scenario is back-swing unstable. In view of this information, the Binary-SIME algorithm switches immediately to a binary search to complete the PTL search, thereby avoiding needless deviations. Therefore, the trajectories of the Binary and Binary-SIME searches are identical in this case.

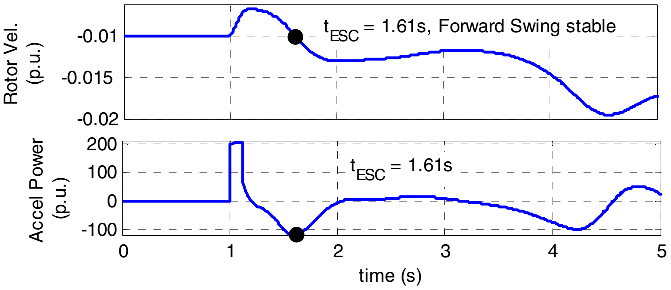

Fig. 12. The OMIB rotor velocity and acceleration power responses for the power transfer of 650MW from VIC. to SA. This response indicates that Case 3 is back-swing unstable.

## VIII. CONCLUSION

The implementation of the enhanced Binary-SIME algorithm, to search for TSLs, using the PSS/E™ software, is described. The implemented TSL searching software provides useful facilities to perform subsidiary investigations from the information generated during a search, for both research and production purposes.

The Binary-SIME algorithm takes advantage of the SIME ESC and limit prediction, to accelerate the search; and switches to binary steps, when the SIME limit prediction fails. It is applied to search for CCTs and PTLs on the IEEE simplified model of the SE Australian Power System. When compared to the binary search method, the results indicate the significant savings in the simulated search time that can be achieved. However, they also reveal limitations of the SIME limit prediction and ESC, particularly in the presence of back-swing instability phenomena due to the limited capacity of SVCs on some interconnectors. In these cases the binary-SIME method does locate the TSL despite the failure of the SIME component of the algorithm. Therefore the binary-SIME method is shown to be more robust than the SIME algorithm, for the cases examined. In such cases, little or no extra time is required by the binary-SIME algorithm as compared to the plain binary search.

The investigation has revealed that enhancements to the ESC are required to identify the occurrence of back-swing instability. It is unclear without further investigation if margin information from forward- and back-swing instability can be utilized for limit prediction within the same search.

The technique for identifying machine groups requires further investigation because there are indications in the cases investigated that some machines may be assigned to an incorrect group. In particular, it may be more appropriate to run the simulation used to identify machine groups for longer than required to detect instability according to the COI angle divergence criterion.

Further investigation of the binary-SIME algorithm including the development of additional enhancements. will be pursued. Such developments will be tested by searching for TSLs in the IEEE Simplified Model of the SE Australian power system, as well as other system models.

## IX. REFERENCES

[1] M. Pavella, D. Ernst, D. Ruiz-Vega, 2000, Transient Stability of Power Systems: A Unified Approach to Assessment and Control, Kluwer Academic Publishers, USA.
[2] H.M. Tan, R. Zivanovic, “Integrating the SIME Method with Standard Time Domain Simulation Software to Search for Transient Stability Limits”, Australian Universities Power Engineering Conference, Sydney, Australia, 2008.
[3] PSS/E Power System Simulator for Engineering, Version 30.2, Siemens Power Transmission & Distribution, Inc., Schenectady, NY, Nov. 2005.
[4] M. Gibbard, D. Vowles, “Simplified 14-Generator Model of the South East Australian Power System”, The School of Electrical & Electronic Engineering, The University of Adelaide, May 2008
http://psdyn.ece.wisc.edu/IEEE_benchmarks
[5] “Python Programming Language -- Official Website”, © 1990-2008, Python Software Foundation, http://www.python.org/.
[6] M. Metcalf, J. Reid, M. Cohen, “Fortran 95/2003 Explained”, Oxford University Press, 2004.
[7] Z. Lan, D.Q. Gan, L.B. Shi, Y.X. Ni and T.S Bi, “Dynamic COI-tracking concept for the control of generators in multi-machine power systems”, Euro. Trans. Electr. Power 2008; John Wiley & Sons, Vol 18, pp 50–64, February 2007
[8] MATLAB ®, The MathWorks Inc., © 1994 – 2009, http://www.mathworks.com.au/.
[9] Y. Zhang, L. Wehenkel, P. Rousseaux and M. Pavella. “SIME: A hybrid approach to fast transient stability assessment and contingency selection”, Electrical Power & Energy Systems, Vol. 19, No. 3, pp. 195- 208, 1997
[10] “SLATEC Common Mathematical Library”, Version 4.1, July 1993, http://www.netlib.org/slatec/
[11] Australian Government, Geoscience Australia, *Maps of Australia – Geoscience Australia*, http://www.ga.gov.au/map, viewed 5 March 2009.

## X. ACKNOWLEDGEMENT

The authors gratefully acknowledge the work of our colleague Dr. Mike Gibbard in developing the simplified model of the SE Australian power system used in the paper.

## XI. BIOGRAPHIES

**Hui-Min Tan** (M’2007) received her Bachelor of Engineer (Electrical and Electronic Engineering), from The University of Adelaide, South Australia, in 2003. She spent 3 years working as a graduate engineer as part of the Power Systems Dynamics Group at the University of Adelaide. Hui-Min commenced her Ph'd in February 2007. Her research interests are in the area of power and control systems engineering.

**David Vowles** (M’96) received a B.Sc. degree, and a B.E.(Hons.) degree in Electrical & Electronic Engineering, from The University of Adelaide, Australia, in 1983 and 1984, respectively. He was employed by the Hydro-Electric Commission of Tasmania in 1984-87 and by Portland Smelter Services, Victoria in 1987-89. From 1993 he has worked as a research engineer at the University.

**Rastko Zivanovic** (M’97) received the Dipl.Ing. and M.Sc. degrees from the University of Belgrade, Belgrade, Serbia, in 1987 and 1991, and the Ph.D. degree from the University of Cape Town, Cape Town, South Africa, in 1997. Currently, he is with the School of Electrical and Electronic Engineering, the University of Adelaide, Australia. His research interests include power system protection and control.